Low-Temperature Heat Capacity and One-Dimensional Ferromagnetic Behavior of the Organic Free Radical 4-Benzylideneamino-2,2,6,6-tetramethylpiperidin-1-oxyl (BATMP)[#]

Takeshi Sakakibara,[†] Yuji Miyazaki,[†] Takayuki Ishida,[§] Takashi Nogami,[§] and Michio Sorai*,[†]

Research Center for Molecular Thermodynamics, Graduate School of Science, Osaka University, Toyonaka, Osaka 560-0043, Japan, and Department of Applied Physics and Chemistry, The University of Electro-Communications, Chofugaoka, Chofu, Tokyo 182-8585, Japan

Received: March 6, 2002

Heat capacities of the organic free radical ferromagnet 4-benzylideneamino-2,2,6,6-tetramethylpiperidin-1-oxyl (BATMP) crystal were measured in the temperature range between 0.1 and 300 K by adiabatic calorimetry. A ferromagnetic phase transition was found at $T_C = 0.19$ K, and a broad heat-capacity anomaly was found arising from the short-range ordering above T_C characteristic of low-dimensional magnetic spin systems. The enthalpy and entropy gains due to both the magnetic phase transition and the heat-capacity anomaly were evaluated to be $\Delta H = 3.86$ J mol^{-1} and $\Delta S = 5.64$ J K^{-1} mol^{-1}, respectively. The value of the experimental magnetic entropy agrees well with the theoretical value R ln 2 (5.76 J K^{-1} mol^{-1}) expected for a spin quantum number $S = {}^1/_2$ spin system (R is the gas constant). The magnetic heat capacity hump due to the short-range order was well accounted for in terms of an $S = {}^1/_2$ one-dimensional ferromagnetic Heisenberg model with the intrachain exchange interaction $J/k_B = 0.95$ K (k_B is Boltzmann's constant). This fact suggests that BATMP crystal is a one-dimensional ferromagnet above T_C. The spin wave analysis of the magnetic heat capacities below T_C revealed that BATMP crystal is in a three-dimensional ferromagnetic state below T_C and the averaged interchain exchange interaction is $J'/k_B = 0.026$ K.

1. Introduction

Development and research on purely organic ferromagnets have been one of the subjects attracting many organic and physical chemists and chemical physicists,[1−7] because one can easily design a variety of molecular and crystal structures in comparison to ordinary magnets such as metals and metal oxides. Furthermore, because most organic magnetic molecules indicate very small magnetic anisotropy, they can be regarded as ideal Heisenberg spin systems, which lead to interesting quantum spin systems. Despite tiny magnetic anisotropy, most organic magnetic crystals exhibit low-dimensional magnetic properties owing to structural anisotropy of constituent molecules.

A class of organic free radicals with 2,2,6,6-tetramethylpiperidin-1-oxyl (TEMPO for short) are typical organic magnets. TEMPO radicals are known to manifest a variety of magnetism by changing the substituent group of TEMPO. Up to now, many TEMPO derivatives have been synthesized and investigated.[8−10]

The TEMPO radical treated here, 4-benzylideneamino-2,2,6,6-tetramethylpiperidin-1-oxyl (abbreviated as BATMP and illustrated in Figure 1), is one of the ferromagnetic TEMPO derivatives. Magnetic measurements of the polycrystalline sample[10c,10d,10f] revealed that BATMP crystal has a positive paramagnetic Curie temperature ($\theta = 0.7$ K) and exhibits a ferromagnetic phase transition at $T_C = 0.18$ K below which a magnetic hysteresis occurs. On the basis of the magnetic susceptibilities above T_C,[10c] the intermolecular exchange interaction parameter was estimated to be $J/k_B = 0.87$ K by the spin quantum number $S = {}^1/_2$ Heisenberg linear chain model and $J/k_B = 2.2$ K by the singlet−triplet model, where k_B denotes Boltzmann's constant. Zero-field muon spin rotation/relaxation/resonance (μSR)[11] indicated that BATMP crystal is a three-dimensional Heisenberg ferromagnet below $T_C = 0.17$ K. X-ray structural analysis and theoretical calculation[10d,12] predicted that BATMP crystal would have a two-dimensional ferromagnetic structure parallel to the *bc* plane.

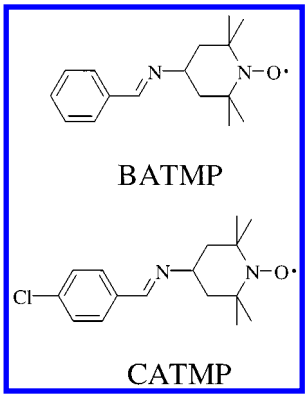

Figure 1. Molecular structure of BATMP and CATMP.

Heat capacity measurement as well as magnetic measurement is a useful tool to investigate magnetic substances. From heat capacities of magnetic materials, one can elucidate the precise magnetic phase transition temperature, spin−spin interaction, magnetic dimensionality, and type of magnetism. Our research group has so far revealed interesting magnetisms of some TEMPO derivative crystals by adiabatic calorimetry.[9a,9b,9d,13,14] The aim of the present work is to elucidate the magnetic properties of the BATMP crystal similar to 4-(4-chlorobenzyli-

[#] Contribution No. 63 from the Research Center for Molecular Thermodynamics.

* To whom correspondence should be addressed. Tel: +81-6-6850-5523. Fax: +81-6-6850-5526. E-mail: sorai@chem.sci.osaka-u.ac.jp.

[†] Osaka University.

[§] The University of Electro-Communications.

10.1021/jp020634n CCC: $22.00
Published on Web 06/05/2002

deneamino)-2,2,6,6-tetramethylpiperidin-1-oxyl (CATMP for short).[10f,10g,15]

2. Experimental Section

Synthesis and purification of BATMP crystal were performed according to the reported method.[10a,10b] The result of elemental analysis of the obtained crystal agreed well with the theoretical values. Calcd for BATMP ($C_{16}H_{23}N_2O$): C, 74.09; H, 8.94; N, 10.80. Found: C, 73.94; H, 8.97; N, 10.79.

In the low-temperature region between 0.1 and 10 K, a very-low-temperature adiabatic calorimeter with a ^{3}He/^{4}He dilution refrigerator[16] was employed, while from 5 to 300 K, an adiabatic microcalorimeter[17] was used. For the very-low-temperature adiabatic calorimeter, 1.254 09 g of the polycrystalline sample was formed into a pellet with a 2 cm diameter and ~2 mm thickness. The pellet was loaded in a gold-plated copper holder with direct thermal contact. For the adiabatic microcalorimeter, 1.341 45 g of the polycrystalline sample was loaded into a gold-plated copper container together with helium gas at ambient pressure to aid thermal equilibration. The true sample masses were derived from buoyancy correction with the sample density, 1.127 g cm^{-3}.[10d]

3. Results and Discussion

A. Heat Capacity. Molar heat capacities at constant pressure, C_p, of BATMP crystal are listed in Table 1 and plotted against temperature, T, in Figure 2. A distinct heat capacity peak due to the ferromagnetic phase transition was observed at $T_C = 0.19$ K, which coincides well with $T_C = 0.18$ K by the magnetic susceptibility measurement[10d,10f] and $T_C = 0.17$ K by the μSR measurement.[11] Furthermore, a heat capacity hump was found in the temperature region centered around 1 K. This thermal anomaly can be regarded as a short-range ordering effect of spins characteristic of low-dimensional magnets.

B. Determination of Lattice and Magnetic Heat Capacities. In general, heat capacities of magnetic substances consist of lattice heat capacities and magnetic heat capacities. We estimated the magnetic heat capacities of BATMP crystal by determining the lattice heat capacity curve and then by subtracting it from the total heat capacities. The observed heat capacities above the magnetic transition temperature can be expressed by the sum of the lattice heat capacities, C_p(lattice), and the magnetic heat capacities due to the short-range order, C_p(short-range). At low temperatures, C_p(lattice) can be approximated by a temperature polynomial with cubic and higher odd powers, while C_p(short-range) may be expressed by a term proportional to T^{-2}.[18] Hence, the total heat capacities, C_p, are given by

$$C_p = C_p(\text{lattice}) + C_p(\text{short-range}) = \sum_{i=1}^{n} c_i T^{2i+1} + c_{n+1} T^{-2} \quad (1)$$

In the present study, we could fit quite well the heat capacity data from 3 to 10 K to eq 1 with $n = 3$: $c_1 = 5.134 \times 10^{-3}$ J K^{-4} mol^{-1}, $c_2 = 2.482 \times 10^{-5}$ J K^{-6} mol^{-1}, $c_3 = -2.391 \times 10^{-7}$ J K^{-8} mol^{-1}, and $c_4 = 3.407$ J K mol^{-1}. The obtained lattice heat capacity curve is shown in Figure 2a by a solid curve.

The excess heat capacities, ΔC_p, arising from the magnetic effect were evaluated by subtraction of the lattice heat capacity from the observed one. Figure 3 shows the plot of ΔC_p against T.

C. Magnetic Enthalpy and Entropy. The magnetic enthalpy and entropy were estimated to be $\Delta H = 3.86$ J mol^{-1} and $\Delta S = 5.64$ J K^{-1} mol^{-1} by integration of the following heat capacities with respect to T and ln T, respectively: (i) spin wave heat capacity below 0.1 K, which will be described later, (ii) the observed magnetic heat capacities between 0.1 and 6.5 K, and (iii) the T^{-2} term in eq 1 from 6.5 K to infinite temperature. This magnetic entropy agrees well with the expected value R ln 2 (5.76 J K^{-1} mol^{-1}) for the magnetic systems with $S = {}^1/_2$ spins, where R is the gas constant. This fact reveals that the present sample really consists of pure organic radical molecules with $S = {}^1/_2$ electron spins.

D. Magnetic Properties. Above T_C, the heat capacity exhibits a remarkable hump centered around 1 K arising from the short-range order of spins characteristic of low-dimensional magnetic systems. In the previous calorimetric study[14] for CATMP crystal having a two-dimensional layer structure,[10g] we revealed that the observed heat capacity anomaly due to the short-range order is reproduced well by the $S = {}^1/_2$ two-dimensional ferromagnetic Heisenberg model of square lattice with the intralayer exchange interaction, $J/k_B = 0.42$ K, where the spin Hamiltonian $H = -2JS_iS_j$ is adopted. Because BATMP crystal has been reported to possess a two-dimensional layer structure[10d] similar to CATMP crystal, one may expect that BATMP crystal would have a two-dimensional magnetic structure. In reality, however, we obtained the result that the magnetic heat capacities between 1 and 5 K are reproduced well by the $S = {}^1/_2$ one-dimensional ferromagnetic Heisenberg model[19] with the intrachain exchange interaction $J/k_B = 0.95$ K rather than by a two-dimensional ferromagnetic Heisenberg model of square lattice. The Padé approximation was used to fit the magnetic heat capacities to the model. The theoretical heat capacity curve thus estimated is drawn in Figure 3 by a solid curve. The present intrachain exchange interaction agrees well with $J/k_B = 0.87$ K estimated by the magnetic susceptibility measurement.[10c]

Next, we discuss the temperature dependence of the magnetic heat capacity below T_C. Magnetic heat capacities of magnetic substances at very low temperatures are generally approximated by the spin wave theory. The heat capacity due to the spin wave (magnon) excitation is proportional to $T^{d/n}$,[20] where d stands for the dimensionality of the magnetic lattice and n is defined as the exponent in the dispersion relation: $n = 1$ for antiferromagnets and $n = 2$ for ferromagnets. To elucidate the nature of the magnetic ordering structure below T_C, we first fitted the following equation to four points of the magnetic heat capacity data at the lowest measurement temperatures:

$$\Delta C_p = aT^{\alpha} \quad (2)$$

The power index α of T was thus estimated to be 1.69. This value is close to ${}^3/_2$, indicating that BATMP crystal is a three-dimensional ferromagnet below T_C. Therefore, we once more fitted eq 2 with $\alpha = {}^3/_2$ to the same data points to yield $a = 51.5$ J K$^{-5/2}$ mol^{-1}. The spin wave heat capacity thus determined is represented in Figure 3 by a broken curve.

Finally, to estimate the value of the interchain exchange interaction, we compared eq 2 with the estimated parameters with the following spin wave heat capacity in three-dimensional ferromagnets possessing nonequivalent spin−spin interaction paths:[13,14]

$$C_{SW} = \frac{5R\zeta({}^5/_2)\Gamma({}^5/_2)}{16\pi^2 S^{3/2}}\left(\frac{k_B{}^3}{2J_1J_2J_3}\right)^{1/2} T^{3/2} \quad (3)$$

where J_1, J_2, and J_3 are the positive exchange interaction parameters for three directions, ζ is Riemann's zeta function,

TABLE 1: Molar Heat Capacities of BATMP Crystal (M = 295.37 g mol^{-1})[a]

T, K	C_p, J K^{-1} mol^{-1}	T, K	C_p, J K^{-1} mol^{-1}	T, K	C_p, J K^{-1} mol^{-1}	T, K	C_p, J K^{-1} mol^{-1}	T, K	C_p, J K^{-1} mol^{-1}
series 1		0.473	1.318	4.335	0.6327	143.27	189.2	10.79	6.557
0.154	2.229	0.504	1.261	4.758	0.7388	145.30	191.5	11.48	7.594
0.163	2.331	0.550	1.241	5.214	0.8883	147.33	193.6	12.20	8.785
0.173	2.930	0.614	1.200	5.609	1.175	149.36	195.9	12.89	9.952
0.186	3.599	0.681	1.183	6.092	1.471	151.89	198.8	13.56	10.83
0.201	2.785	0.755	1.157	6.515	1.681	154.91	202.1	14.23	12.12
0.212	2.416	0.835	1.143	6.919	2.049	157.93	205.3	14.94	13.61
0.233	2.222			7.497	2.589	160.95	208.6	15.64	14.66
0.261	1.864	series 6		8.185	3.278	163.97	212.0	16.39	16.03
0.290	1.667	0.185	3.504	8.923	4.138	167.00	215.3	17.15	17.36
0.321	1.533	0.196	2.848	9.723	4.910	170.02	218.5	17.93	18.94
0.353	1.495	0.209	2.689			173.05	221.6	18.71	20.56
0.395	1.378	0.225	2.226	series 9		176.07	225.0	19.51	22.12
0.452	1.286	0.240	2.118	1.173	1.030	179.09	228.4	20.35	23.42
0.517	1.254	0.258	1.939	1.327	0.9567	182.12	231.6	21.25	25.35
0.585	1.205	0.274	1.813	1.510	0.8912	185.15	234.8	22.22	27.30
0.660	1.171	0.292	1.722	1.702	0.8231	188.17	238.0	23.26	29.16
0.735	1.160	0.312	1.655	1.921	0.7643	191.20	241.4	24.49	31.44
0.818	1.130	0.334	1.536	2.164	0.6814	194.23	244.7	25.84	34.02
0.909	1.098	0.361	1.467	2.460	0.5934	197.25	247.8	27.20	36.37
1.002	1.086	0.394	1.389	2.750	0.5334	200.28	251.2	28.58	38.88
1.139	1.031	0.427	1.342	3.072	0.5099	203.31	254.4	29.96	41.51
1.274	0.9746	0.463	1.303	3.389	0.5103	206.34	257.5	31.38	43.51
1.442	0.9156	0.500	1.256	3.734	0.5301	209.37	260.9	32.79	46.04
1.662	0.8096			4.103	0.5906	212.40	264.1	34.20	48.57
1.882	0.7352	series 7		4.507	0.6616	215.43	267.0	35.62	50.70
		0.169	2.867	4.940	0.7968	218.45	270.1	37.05	52.95
series 2		0.178	3.247	5.408	0.9670	221.48	273.5	38.48	55.34
0.254	1.816	0.188	3.279	5.891	1.219	224.51	276.9	39.92	57.56
0.285	1.778	0.199	2.881	6.428	1.573	227.53	280.2	41.37	60.19
0.317	1.629	0.214	2.581	7.045	2.013	230.56	283.3	42.82	62.12
0.352	1.511	0.231	2.249	7.713	2.595	233.59	286.6	44.28	64.22
0.389	1.445	0.248	1.928	8.434	3.325	236.61	289.8	45.74	66.54
0.426	1.350	0.274	1.825	9.214	4.225	239.64	292.9	47.20	68.26
0.463	1.283	0.310	1.644	10.06	4.980	242.66	296.1	48.67	70.35
0.501	1.251	0.351	1.513			245.69	299.6	50.14	72.69
0.541	1.256	0.395	1.402	series 10		248.71	303.2	51.85	75.02
0.602	1.184	0.443	1.323	80.81	113.6	251.74	306.2	53.78	77.92
0.678	1.174	0.495	1.265	82.74	115.8	254.76	309.5	55.71	80.66
		0.534	1.274	84.74	118.4	257.79	313.0	57.66	83.27
series 3		0.586	1.198	86.74	121.2	260.81	316.4	59.60	85.87
0.147	2.023	0.651	1.172	88.74	123.8	263.83	319.9	61.56	88.55
0.164	2.508	0.719	1.155	90.74	126.3	266.86	323.2	63.52	91.04
0.179	3.226	0.772	1.135	92.75	128.9	269.88	326.2	65.48	93.78
0.188	3.128	0.845	1.125	94.76	131.5	272.90	329.6	67.44	96.48
0.196	3.084	0.947	1.090	96.76	133.9	275.90	333.9	69.41	98.69
0.211	2.516	1.056	1.052	98.77	136.6	278.89	337.6	71.38	101.4
0.223	2.331	1.171	1.020	100.79	139.4	281.89	341.0	73.36	103.9
0.241	2.094	1.308	0.9616	102.80	141.8	284.88	344.6	75.33	106.5
0.290	1.752	1.470	0.8934	104.81	144.4	287.88	348.0	77.31	109.1
0.343	1.508	1.647	0.8127	106.83	147.0	290.87	351.6	79.30	111.8
		1.921	0.7075	108.85	149.4	293.87	354.8	81.28	114.3
series 4				110.86	151.9	296.86	357.9	83.26	117.0
0.227	2.329	series 8		112.88	154.3	299.86	362.1	85.25	119.8
0.248	1.967	0.954	1.123	114.90	156.5			87.24	122.3
0.272	1.787	1.100	1.074	116.93	159.0	series 11		89.23	125.0
0.297	1.620	1.241	1.014	118.95	161.4	5.475	1.040	91.23	127.5
		1.395	0.9724	120.97	163.9	5.649	1.195	93.22	130.1
series 5		1.572	0.8807	122.99	166.4	5.901	1.315	95.21	132.6
0.243	2.000	1.723	0.8126	125.02	168.5	6.244	1.474	97.21	135.4
0.265	1.870	1.884	0.7653	127.04	170.7	6.622	1.649	99.21	137.6
0.289	1.698	2.083	0.6868	129.07	173.1	7.056	2.062		
0.313	1.639	2.338	0.6104	131.10	175.3	7.518	2.566		
0.336	1.547	2.624	0.5720	133.12	177.5	8.010	3.057		
0.361	1.489	2.923	0.5192	135.15	179.9	8.496	3.526		
0.387	1.463	3.238	0.5079	137.18	182.2	8.982	4.073		
0.416	1.377	3.572	0.5182	139.21	184.5	9.518	4.817		
0.444	1.317	3.940	0.5574	141.24	186.8	10.12	5.587		

[a] Data in series 1−9 and series 10 and 11 were collected by use of different adiabatic calorimeters.

Γ is Euler's gamma function, and S is the spin quantum number. In this case, $J_1 = J = 0.95k_B$ K, $J_2 = J_3 = J'$, which is an averaged interchain exchange interaction, and $S = {}^1/_2$. As a result, comparison of eq 2 with eq 3 yielded $J'/k_B = 0.026$ K.

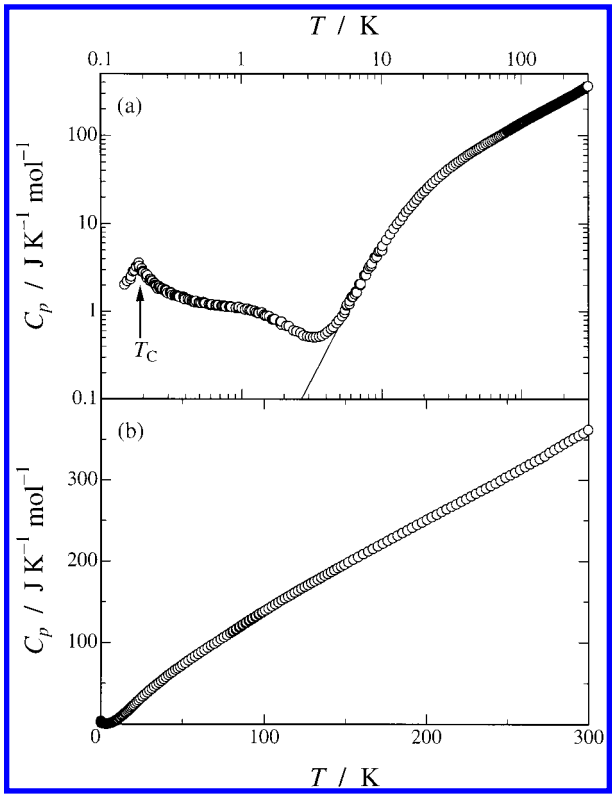

Figure 2. Molar heat capacities of BATMP crystal on (a) logarithmic and (b) normal scales. Solid curve indicates estimated lattice heat capacity.

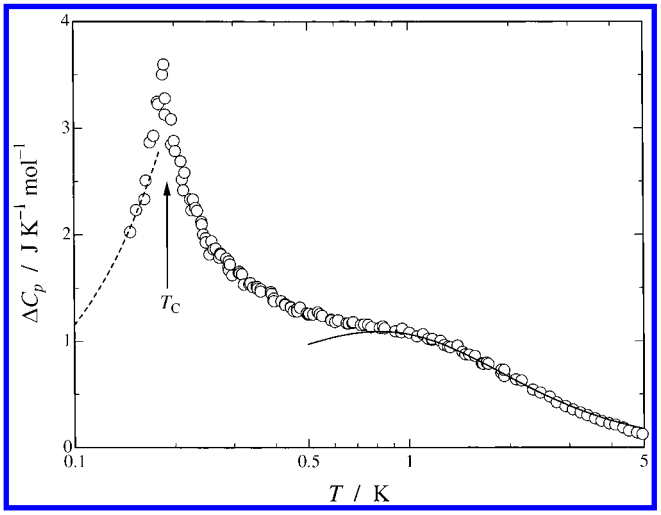

Figure 3. Magnetic heat capacities of BATMP crystal. Solid curve indicates the heat capacity calculated from high-temperature series expansion for $S = {}^1/_2$ one-dimensional ferromagnetic Heisenberg model with $J/k_B = 0.95$ K. Broken curve shows the heat capacity derived from spin wave theory for three-dimensional ferromagnets.

For a possible mechanism of the ferromagnetic interaction working between the N−O radicals of adjacent TEMPO moieties in some TEMPO radical crystals, Nogami et al.[10g,12] proposed the β-hydrogen mechanism that a positive spin on the N−O radical induces negative spins on the β-hydrogen atoms due to an intramolecular spin polarization, such as ON(↑)−C_α(↓)−C_β(↑)−H_β(↓), inducing a positive spin on the N−O sites of the adjacent molecules in turn. They expected two-dimensional magnetic network structures for four ferromagnetic TEMPO derivative crystals Ar−CH═N−TEMPO (Ar = phenyl, 4-(methylthio)phenyl, 4-chlorophenyl, and 4-biphenylyl) on the basis of the distance between the N−O radicals of the adjacent molecules by the X-ray structural analyses.[10d,10e,10g,10j,12] Actually, we revealed that CATMP (Ar = 4-chlorophenyl) crystal exhibits two-dimensional ferromagnetism above T_C by the heat capacity experiment.[14] In the present case, however, we elucidate that BATMP crystal is characterized not by two-dimensional but by one-dimensional magnets. A few possible reasons for that are considered. One is that the magnitude of the exchange interaction between the N−O radicals of the adjacent TEMPO moieties decreases rapidly as the distance between the N−O radicals increases. In CATMP crystal, the O···O distances along the *a* and *c* axes are 5.91 and 5.95 Å, respectively,[10g] which are substantially equal within ∼0.7%. On the other hand, in BATMP crystal, the O···O distances along the *b* and *c* axes are 6.15 and 5.62 Å, respectively,[10d] the difference of which is as large as 9%. In A_2CuX_4 and $A'CuX_4$ compounds (A, A′ are mono- and divalent nonmagnetic cations; X is a halide anion), actually, the magnitude of the exchange interaction between the CuX_4^{2-} ions decreases exponentially as the X···X distance increases.[21] Another possibility is that the paths of the exchange interaction for both crystals are different because of the difference of the crystal structure. CATMP crystal possesses a parallel arrangement of the N−O groups along the *a* axis and a zigzag arrangement of the N−O groups along the *c* axis in the two-dimensional sheet,[10g] whereas BATMP crystal has only a zigzag arrangement of the N−O groups along the *b* and *c* axes.[10d] The difference of the arrangement of the N−O group for both crystals causes the different intermolecular atomic contacts and consequently different magnitudes of exchange interaction on the basis of the β-hydrogen mechanism. In fact, distances of O···H(axial methyl) and O···H(equatorial methyl) are the shortest in the *c* and *a* axis directions, respectively, within a sheet arrangement of BATMP. On the other hand, distances of O···H(methylene) and O···H(equatorial methyl) are shortest in the *b* and *c* axis directions, respectively, for CATMP. The experimental results suggest that one of the two intrasheet exchange interactions in BATMP is negligible above T_C, while both intrasheet interactions are appreciable above T_C for CATMP.

From comparison between eqs 2 and 3, we could estimate the averaged interchain exchange interaction $J'/k_B = 0.026$ K. Because of the difference between the O···O distances along the *a* and *b* axes (11.89 and 6.15 Å, respectively), however, the interchain exchange interactions along the *a* and *b* axes would be rather different. In the case of CATMP crystal, the interchain exchange interaction along the *c* axis was estimated to be $J'/k_B = 0.024$ K,[14] which corresponds to the exchange interaction working between the N−O radicals with the O···O distance of 10.86 Å.[10g] Therefore, the exchange interaction along the *a* axis for BATMP crystal is expected to be smaller than that along the *c* axis for CATMP crystal.

4. Conclusions

Heat capacities of the organic ferromagnet BATMP radical crystal were measured from 0.1 to 300 K by adiabatic calorimetry. A heat capacity peak due to a ferromagnetic phase transition was observed at $T_C = 0.19$ K. Above T_C, a heat capacity hump was also found, which arises from the short-range order of the spins characteristic of low-dimensional magnetic materials. The magnetic enthalpy and entropy were evaluated to be $\Delta H = 3.86$ J mol^{-1} and $\Delta S = 5.64$ J K^{-1} mol^{-1}, respectively. The experimental magnetic entropy is in good agreement with the expected value R ln 2 (5.76 J K^{-1} mol^{-1}) for $S = {}^1/_2$ spin systems. Contrary to the prediction that the BATMP crystal possesses a similar two-dimensional crystal

structure[10d] to that in CATMP crystal,[10g] BATMP crystal exhibits one-dimensional ferromagnetism above T_C. The magnetic heat capacity hump due to the short-range order was reproduced well by the $S = {}^1/_2$ one-dimensional ferromagnetic Heisenberg model with the intrachain exchange interaction $J/k_B = 0.95$ K. The spin wave analysis of the magnetic heat capacities below T_C revealed that the BATMP crystal orders into a three-dimensional ferromagnetic state below T_C and has the averaged interchain exchange interaction $J'/k_B = 0.026$ K.

In this work, we showed that a slight difference of the crystal structures in TEMPO derivative radicals affects their magnetism dramatically. If we measure the heat capacities of 4-(4-methylthiobenzylideneamino)-TEMPO[10j] and 4-(4-phenylbenzylideneamino)-TEMPO[10e] radical crystals, which are isomorphous to the BATMP crystal[10d] and CATMP crystal,[10g] respectively, we would gain a useful clue to elucidate the mechanism of their magnetic dimensionality more clearly.

References and Notes

(1) *Magnetic Molecular Materials*; Gatteschi, D., Kahn, O., Miller, J. S., Palacio, F., Eds.; NATO ASI Series E; Kluwer Academic Publishers: Dordrecht, 1991; Vol. 198.

(2) Kahn, O. *Molecular Magnetism*; Wiley-VCH: New York, 1993.

(3) *Magnetism: A Supramolecular Function*; Kahn, O., Ed.; NATO ASI Series C; Kluwer Academic Publishers: Dordrecht, 1996; Vol. 484.

(4) *Molecular Magnetism: From Molecular Assemblies to the Devices*; Coronado, E., Delhaès, P., Gatteschi, D., Miller, J. S., Eds.; NATO ASI Series E; Kluwer Academic Publishers: Dordrecht, 1996; Vol. 321.

(5) *Molecule-Based Magnetic Materials: Theory, Techniques, and Applications*; Turnbull, M. M., Sugimoto, T., Thompson, L. K., Eds.; ACS Symposium Series 644; American Chemical Society: Washington, DC, 1996.

(6) *Magnetic Properties of Organic Materials*; Lahti, P. M., Ed.; Marcel Dekker: New York, 1999.

(7) *Molecular Magnetism: New Magnetic Materials*; Ito, K., Kinoshita, M., Eds.; Kodansha & Gordon and Breach Science Publishers: Tokyo & Amsterdam, 2000.

(8) Bordeaux, P. D.; Lajzerowicz, J. *Acta Crystallogr. B* **1977**, *33*, 1837.

(9) (a) Sugimoto, H.; Aota, H.; Harada, A.; Morishima, Y.; Kamachi, M.; Mori, W.; Kishita, M.; Ohmae, N.; Nakano, M.; Sorai, M. *Chem. Lett.* **1991**, 2095. (b) Kamachi, M.; Sugimoto, H.; Kajiwara, A.; Harada, A.; Morishima, Y.; Mori, W.; Ohmae, N.; Nakano, M.; Sorai, M.; Kobayashi, T.; Amaya, K. *Mol. Cryst. Liq. Cryst.* **1993**, *232*, 53. (c) Kajiwara, A.; Sugimoto, H.; Kamachi, M. *Bull. Chem. Soc. Jpn.* **1994**, *67*, 2373. (d) Kajiwara, A.; Mori, W.; Sorai, M.; Yamaguchi, K.; Kamachi, M. *Mol. Cryst. Liq. Cryst.* **1995**, *272*, 67.

(10) (a) Ishida, T.; Tomioka, K.; Nogami, T.; Iwamura, H.; Yamaguchi, K.; Mori, W.; Shirota, Y. *Mol. Cryst. Liq. Cryst.* **1993**, *232*, 99. (b) Tomioka, K.; Ishida, T.; Nogami, T.; Iwamura, H. *Chem. Lett.* **1993**, 625. (c) Tomioka, K.; Mitsubori, S.; Ishida, T.; Nogami, T.; Iwamura, H. *Chem. Lett.* **1993**, 1239. (d) Nogami, T.; Tomioka, K.; Ishida, T.; Yoshikawa, H.; Yasui, M.; Iwasaki, F.; Iwamura, H.; Takeda, N.; Ishikawa, M. *Chem. Lett.* **1994**, 29. (e) Ishida, T.; Tsuboi, H.; Nogami, T.; Yoshikawa, H.; Yasui, M.; Iwasaki, F.; Iwamura, H.; Takeda, N.; Ishikawa, M. *Chem. Lett.* **1994**, 919. (f) Nogami, T.; Ishida, T.; Yoshikawa, H.; Yasui, M.; Iwasaki, F.; Iwamura, H.; Takeda, N.; Ishikawa, M. *Synth. Met.* **1995**, *71*, 1813. (g) Nogami, T.; Ishida, T.; Tsuboi, H.; Yoshikawa, H.; Yamamoto, H.; Yasui, M.; Iwasaki, F.; Iwamura, H.; Takeda, N.; Ishikawa, M. *Chem. Lett.* **1995**, 635. (h) Ishida, T.; Tomioka, K.; Nogami, T.; Yoshikawa, H.; Yasui, M.; Iwasaki, F.; Takeda, N.; Ishikawa, M. *Chem. Phys. Lett.* **1995**, *247*, 7. (i) Yasui, M.; Yoshikawa, H.; Yamamoto, H.; Ishida, T.; Nogami, T.; Iwasaki, F. *Mol. Cryst. Liq. Cryst.* **1996**, *279*, 77. (j) Nogami, T.; Ishida, T.; Yasui, M.; Iwasaki, F.; Iwamura, H.; Takeda, N.; Ishikawa, M. *Mol. Cryst. Liq. Cryst.* **1996**, *279*, 97. (k) Togashi, K.; Imachi, R.; Tomioka, K.; Tsuboi, H.; Ishida, T.; Nogami, T.; Takeda, N.; Ishikawa, M. *Bull. Chem. Soc. Jpn.* **1996**, *69*, 2821. (l) Nogami, T.; Imachi, R.; Ishida, T.; Takeda, N.; Ishikawa, M. *Mol. Cryst. Liq. Cryst.* **1997**, *305*, 211. (m) Iwasaki, F.; Yoshikawa, J. H.; Yamamoto, H.; Kan-nari, E.; Takada, K.; Yasui, M.; Ishida, T.; Nogami, T. *Acta Crystallogr. B* **1999**, *55*, 231. (n) Iwasaki, F.; Yoshikawa, J. H.; Yamamoto, H.; Takada, K.; Kan-nari, E.; Yasui, M.; Ishida, T.; Nogami, T. *Acta Crystallogr. B* **1999**, *55*, 1057.

(11) Ishida, T.; Ohira, S.; Ise, T.; Nakayama, K.; Watanabe, I.; Nogami, T.; Nagamine, K. *Chem. Phys. Lett.* **2000**, *330*, 110.

(12) Nogami, T.; Ishida, T.; Yasui, M.; Iwasaki, F.; Takeda, N.; Ishikawa, M.; Kawakami, T.; Yamaguchi, K. *Bull. Chem. Soc. Jpn.* **1996**, *69*, 1841.

(13) Ohmae, N.; Kajiwara, A.; Miyazaki, Y.; Kamachi, M.; Sorai, M. *Thermochim. Acta* **1995**, *267*, 435.

(14) Miyazaki, Y.; Matsumoto, T.; Ishida, T.; Nogami, T.; Sorai, M. *Bull. Chem. Soc. Jpn.* **2000**, *73*, 67.

(15) Imachi, R.; Ishida, T.; Nogami, T.; Ohira, S.; Nishiyama, K.; Nagamine, K. *Chem. Lett.* **1997**, 233.

(16) Murakawa, S.; Wakamatsu, T.; Nakano, M.; Sorai, M.; Suga, H. *J. Chem. Thermodyn.* **1987**, *19*, 1275.

(17) Kume, Y.; Miyazaki, Y.; Matsuo, T.; Suga, H. *J. Phys. Chem. Solids* **1992**, *53*, 1297.

(18) Blöte, H. M. J. *Physica B* **1975**, *79*, 427.

(19) de Neef, T.; Kuipers, A. J. M.; Kopinga, K. *J. Phys. A* **1974**, *7*, L171.

(20) de Jongh, L. J.; Miedema, A. R. *Adv. Phys.* **1974**, *23*, 1.

(21) Willett, R. D.; Place, H.; Middleton, M. *J. Am. Chem. Soc.* **1988**, *110*, 8639.